Can oxygen stable isotopes be used to track precipitation moisture source in vascular plant-dominated peatlands?

CrossMark

Matthew J. Amesbury [a,*], Dan J. Charman [a], Rewi M. Newnham [b], Neil J. Loader [c], Jordan Goodrich [d,e], Jessica Royles [f], David I. Campbell [d], Elizabeth D. Keller [g], W. Troy Baisden [g], Thomas P. Roland [a], Angela V. Gallego-Sala [a]

[a] Geography, College of Life and Environmental Sciences, University of Exeter, Exeter, UK
[b] School of Geography, Earth and Environmental Sciences, Victoria University of Wellington, Wellington, New Zealand
[c] Department of Geography, College of Science, Swansea University, Swansea, UK
[d] School of Science, University of Waikato, Hamilton, New Zealand
[e] Global Change Research Group, San Diego State University, San Diego, USA
[f] Department of Plant Sciences, University of Cambridge, Cambridge, UK
[g] National Isotope Centre, GNS Science, Lower Hutt, Wellington, New Zealand

ARTICLE INFO

ABSTRACT

Variations in the isotopic composition of precipitation are determined by fractionation processes which occur during temperature- and humidity-dependent phase changes associated with evaporation and condensation. Oxygen stable isotope ratios have therefore been frequently used as a source of palaeoclimate data from a variety of proxy archives, which integrate this signal over time. Applications from ombrotrophic peatlands, where the source water used in cellulose synthesis is derived solely from precipitation, have been mostly limited to Northern Hemisphere *Sphagnum*-dominated bogs, with few in the Southern Hemisphere or in peatlands dominated by vascular plants. New Zealand (NZ) provides an ideal location to undertake empirical research into oxygen isotope fractionation in vascular peatlands because single taxon analysis can be easily carried out, in particular using the preserved root matrix of the restionaceous wire rush (*Empodisma* spp.) that forms deep Holocene peat deposits throughout the country. Furthermore, large gradients are observed in the mean isotopic composition of precipitation across NZ, caused primarily by the relative influence of different climate modes. Here, we test whether δ^{18}O of *Empodisma* α-cellulose from ombrotrophic restiad peatlands in NZ can provide a methodology for developing palaeoclimate records of past precipitation δ^{18}O. Surface plant, water and precipitation samples were taken over spatial (six sites spanning $>10°$ latitude) and temporal (monthly measurements over one year) gradients. A link between the isotopic composition of root-associated water, the most likely source water for plant growth, and precipitation in both datasets was found. Back-trajectory modelling of precipitation moisture source for rain days prior to sampling showed clear seasonality in the temporal data that was reflected in root-associated water. The link between source water and plant cellulose was less clear, although mechanistic modelling predicted mean cellulose values within published error margins for both datasets. Improved physiological understanding and modelling of δ^{18}O in restiad peatlands should enable use of this approach as a new source of palaeoclimate data to reconstruct changes in past atmospheric circulation.

© 2015 The Authors. Published by Elsevier B.V. This is an open access article under the CC BY license (http://creativecommons.org/licenses/by/4.0/).

1. Introduction

Variations in the stable isotopic composition of precipitation (δ^{18}O and δD) are determined by multiple fractionation processes which occur during temperature- and humidity-dependent phase changes associated with evaporation and condensation (Dansgaard, 1964; Craig and Gordon, 1965; Gat, 2000). The isotopic composition of precipitation is also known to reflect rainout history and atmospheric circulation patterns along given air mass trajectories (Cole et al., 1999; Araguas-Araguas et al., 2000). The subsequent incorporation of this signal into plants, sediments and ice has led to the use of oxygen stable isotope ratios (δ^{18}O) for palaeoclimate reconstructions from a variety of proxy archives including tree rings, lakes, speleothems (see Leng, 2004 and references therein), ice cores (Brook, 2007) and, less frequently, in peatlands. Ex-

ploitation of the δ^{18}O record from ombrotrophic peatlands, where the source water used in cellulose synthesis is derived solely from precipitation, has been mostly limited to Northern Hemisphere *Sphagnum*-dominated bogs (e.g. Brenninkmeijer et al., 1982; Ménot-Combes et al., 2002; Zanazzi and Mora, 2005; Daley et al., 2010). There has been limited application in the Southern Hemisphere (SH; Royles et al., 2013) or in vascular plant-dominated peatlands (Hong et al., 2000, 2009), despite considerable potential for such records to improve understanding of SH climate dynamics.

The oxygen stable isotope content of vascular plant cellulose ($\delta^{18}O_C$) is determined by kinetic and equilibrium fractionation pathways from source water (Barbour, 2007). Leaf water is used for sucrose synthesis in plants and is generally isotopically enriched relative to meteoric source water ($\delta^{18}O_{SW}$) due to evaporative enrichment during transpiration (Yakir and DeNiro, 1990; Buhay et al., 1996). $\delta^{18}O_C$ depends on both the isotopic composition of the sucrose and that of the water at the site of cellulose synthesis, which may be spatially and temporally separated from sucrose synthesis. Models to describe these fractionation processes and predict $\delta^{18}O_C$ from $\delta^{18}O_{SW}$ have been developed, initially for trees (e.g. Waterhouse et al., 2002), but have been widely applied, including to peatlands dominated by different vegetation types (e.g. Ménot-Combes et al., 2002; Zanazzi and Mora, 2005; Daley et al., 2010). Vascular and non-vascular plants record different δ^{18}O from a given water source (Ménot-Combes et al., 2002; Nichols et al., 2010), largely due to the presence/absence respectively of stomata capable of regulating moisture/gas exchange. In addition, although $\delta^{18}O_C$ records have previously been interpreted as 'palaeo-thermometers' driven by surface air temperature (e.g. Hong et al., 2000), this link is indirect (Barbour, 2007), can be complicated by the uncoupling of air and leaf temperatures (Helliker and Richter, 2008) and is often untested (e.g. Oldfield, 2001). Quantitative palaeo-temperature estimates from peatland $\delta^{18}O_C$ data are therefore problematic and instead, $\delta^{18}O_C$ has been interpreted as a proxy for precipitation moisture source (Daley et al., 2010). If palaeoclimate indices are developed from $\delta^{18}O_C$ records in novel geographical or ecological contexts, it is critical that relationships between the isotopic compositions of precipitation, source waters and plant cellulose are empirically and mechanistically grounded and calibrated with modern climate data (e.g. Daley et al., 2012), or understood via probabilistic statistical approaches such as inverse proxy modelling (Yu et al., 2011; Yu, 2013).

The primary influences on the stable oxygen isotopic composition of plant cellulose are 1) the isotopic composition of source water and of water at the site of cellulose synthesis; 2) isotopic enrichment of water in the leaf due to evaporation (i.e. equilibrium and kinetic physical fractionation effects); and 3) biochemical fractionations during cellulose synthesis. Whilst physical fractionation effects are temperature- and humidity-dependent, the biochemical fractionation of 27 ± 3‰ (Yakir and DeNiro, 1990; Aucour et al., 1996) has generally been considered to be independent of temperature, although some evidence exists to the contrary (Sternberg and Ellsworth, 2011). In studies of $\delta^{18}O_C$ from *Sphagnum*-dominated peatlands, physical fractionation processes have been disregarded due to the simpler physiological water-use strategies of mosses compared to vascular plants, such that only a biochemical fractionation factor has been applied to test the link between moss cellulose and $\delta^{18}O_{SW}$ (Daley et al., 2010).

Throughout NZ, ombrotrophic peatlands are dominated by the restionaceous wire rush (*Empodisma minus* and *Empodisma robustum*; Wagstaff and Clarkson, 2012). Both species, occurring separately north and south of 38°S (known as the 'Kauri Line'), have reduced, scale-like leaves, high water-use efficiency, a surface cluster root matrix with a similar base exchange and water holding capacity to *Sphagnum*, can reduce water loss via stomatal control
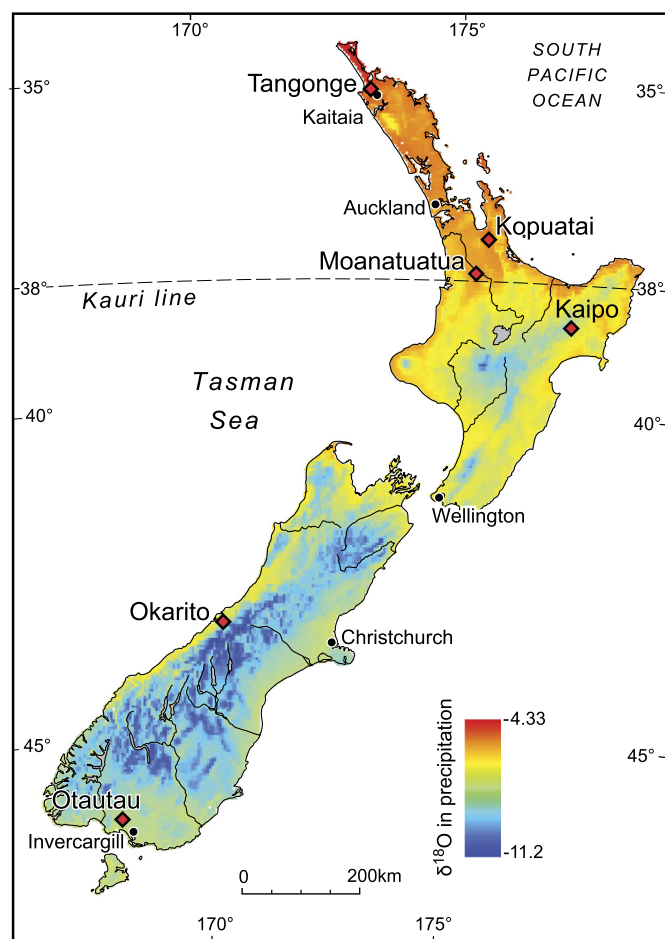

Fig. 1. Site locations. Kauri line represents geographical split of the two *Empodisma* species *E. robustum* (to the north of 38°) and *E. minus* (to the south of 38°) (Wagstaff and Clarkson, 2012). Base map is isoscape modelled annually-weighted 1997–2013 mean δ^{18}O in precipitation (‰; see Section 2.2 for details) generated using the relationships reported in Table S1. For a full colour version of this figure, the reader is referred to the web version of this article.

and form a dense canopy of standing living and dead shoots, reducing rates of surface evaporation (Agnew et al., 1993; Campbell and Williamson, 1997; Wagstaff and Clarkson, 2012). NZ is therefore an ideal location to develop understanding of oxygen isotope fractionation in vascular plant peatlands because the dominance of a single taxon in both surface vegetation and peat avoids mixed species effects (Ménot-Combes et al., 2002; Nichols et al., 2010). Many of the peatlands also preserve high-resolution full-Holocene sequences (e.g. Newnham et al., 1995; Vandergoes et al., 2005) and are situated in the climatically sensitive SH mid-latitudes (e.g. Ummenhofer and England, 2007; Fletcher and Moreno, 2012). Crucially, large gradients exist in the annual mean isotopic composition of precipitation across NZ (Fig. 1), caused primarily by the relative influence of northern and southern air masses driven by different climate modes (e.g. ENSO and the southern westerlies, driven by the Southern Annular Mode; Ummenhofer and England, 2007), as well as altitude and rainout effects across inland areas.

Here, we test the potential for δ^{18}O in ombrotrophic restiad peatlands to provide a basis for developing palaeoclimatic records that track precipitation moisture source. Specifically, we test the following hypotheses:

H1: The oxygen stable isotopic composition of the source water ($\delta^{18}O_{SW}$) used by *Empodisma* spp. in cellulose synthesis tracks the isotopic composition of precipitation, both spatially and temporally.

H2: The oxygen stable isotopic composition of the peat forming parts of *Empodisma* spp. ($\delta^{18}O_C$; i.e. the cluster root matrix; Wagstaff and Clarkson, 2012) reflect spatial and temporal variation in the source water, subject to fractionation and enrichment effects.

2. Methods

2.1. Sites and field sampling

Six *Empodisma*-dominated ombrotrophic peatlands were selected to span variability in the isotopic gradient of precipitation across NZ (Fig. 1, Table 1). Divided by the Kauri Line, the three northern sites, Tangonge (TNG), Kopuatai (KOP) and Moanatuatua (MOA) contain *E. robustum* whereas the three southern sites, Kaipo (KAI), Okarito (OKA) and Otautau (OTT), contain *E. minus* (Wagstaff and Clarkson, 2012). All sites have been defined as ombrotrophic (e.g. Newnham et al., 1995; Elliot, 1998; Newnham and Lowe, 2000; Campbell et al., 2014) or display characteristics associated with ombrotrophy, such as typically diagnostic vegetation communities, domed or raised profiles in relation to surrounding land and an acidic substrate. This selection criteria was applied to provide confidence that the only water source available to plants was precipitation, though we acknowledge that our sites fall on a gradient from those where we can be very confident of ombrotrophy (KOP, MOA), to intermediate sites where less information is available (TNG, OKA, OTT) to one site where, given its topographic setting, the influence of other water sources must be deemed a possibility (KAI).

We employed both spatial and temporal approaches to sampling and analysis. For the spatial approach, we sampled six locations on each site in November 2012, providing a total dataset of 36 sampling points. At each sampling point, we took two *Empodisma* spp. plant samples (surface cluster roots and recent shoot growth), two potential external source water samples (one squeezed from the interstitial cluster root water, hereafter referred to as 'root-associated water' and one from the below ground watertable, hereafter referred to as 'bog water' – see Table 2 for mean, minimum and maximum bog water sampling depths) and a watertable depth measurement to test the potential effect of microtopography on evaporative enrichment (Ménot-Combes et al., 2002). Sampling root-associated water provides only an approximation of the internal root water but we use it here in addition to precipitation to examine potential sources of external source water. We also took plant samples of recent growth of the most common other plant species present at each site, including *Sphagnum* spp., *Machaerina teretifolia*, *Gleichenia dicarpa*, *Leptospermum scoparium* and *Dracophyllum longifolium*.

For the temporal approach, aimed at understanding seasonal changes, we took monthly samples of root and recent shoot growth, root-associated and bog water and monthly integrated precipitation at two locations on one site (KOP) from November 2012 to November 2013. Precipitation over the year was measured using a tipping bucket rain gauge (TB5, Hydrological Services, NSW, Australia) situated 0.8 m (mean canopy height) above the surface. Wind direction was measured with a three dimensional sonic anemometer (CSAT3, Campbell Scientific, Utah, USA) mounted on a tower 4.25 m above the peat surface with continuous half-hourly wind statistics collected and stored on a data logger (CR3000, Campbell Scientific, Utah, USA), with daily (24 h) means calculated for analysis.

2.2. Climate and isoscape data and modelling

Climate data for mean monthly temperature, total monthly precipitation and monthly relative humidity were downloaded from the NZ National Institute for Water and Atmospheric Research

Table 1
Site data. Climate data for temperature, precipitation and relative humidity was downloaded from the NIWA Virtual Climate Station Network, see text for details. Isoscape values for $\delta^{18}O$ and δD in precipitation (ppt) are annual means from 1972–1991 for Kaitaia (TNG) and 1977–1991 for Invercargill (OTT). SD = standard deviation. GNIP values for $\delta^{18}O$ and δD in precipitation (ppt) are annual means from 1997 to 2012. GNIP values for $\delta^{18}O$ and δD in precipitation (ppt) are annual means from 1997 to 2012.

Site	Region	Lat (°S)	Long (°E)	Altitude (m)	*Empodisma* species	Temperature (°C) Mean annual	Temperature (°C) Mean summer	Precipitation (mm) Total annual	Precipitation (mm) Total summer	Relative humidity (%)	Isoscape mean annual $\delta^{18}O$ in ppt (SD)	GNIP mean annual $\delta^{18}O$ in ppt (SD)	Isoscape mean annual δD in ppt (SD)	GNIP mean annual δD in ppt (SD)
TNG	Northland	35.1048	173.2156	10	*E. robustum*	15.85	19.21	1318	259	84.9	−4.32 (1.16)	−4.48 (0.93)	−23.18 (6.94)	−24.28 (5.71)
KOP	Waikato	37.3879	175.5552	5	*E. robustum*	14.72	19.05	1186	242	80.5	−5.09 (1.23)	–	−30.35 (7.95)	–
MOA	Waikato	37.9235	175.3701	60	*E. robustum*	13.63	18.04	1186	256	82.8	−5.29 (1.23)	–	−30.46 (7.81)	–
KAI	Te Urewera National Park	38.6849	1772011	1000	*E. minus*	9.96	14.70	2665	521	82.4	−7.32 (1.04)	–	−44.81 (8.17)	–
OKA	West Coast	43.2471	170.2205	75	*E. minus*	11.72	15.19	3338	887	84.3	−6.53 (1.18)	–	−43.62 (8.05)	–
OTT	Southland	46.1311	168.0324	65	*E. minus*	9.98	14.09	1053	276	82.8	−7.34 (1.34)	−7.01 (0.76)	−50.37 (10.23)	−47.39 (4.64)

Table 2

Mean values and ranges of root-associated and bog water $\delta^{18}O(‰)$ and water table depth for all sites in the spatial dataset. WTD = water table depth.

Site	Mean (‰)		Range (‰)		WTD mean (cm)	WTD range (min–max, cm)
	Root water	Bog water	Root water	Bog water		
TNG	−3.3	−5.9	1.3	1.6	30.5	7 (27–34)
KOP	−1.6	−6.1	4.4	2.3	8.3	8 (4–12)
MOA	−4.5	−5.3	2.1	0.6	59.7	23 (50–73)
KAI	−4.4	−5.3	2.3	2.2	19.3	24 (5–29)
OKA	−4.8	−4.7	1.1	1.4	2.5	16 (−5*–11)
OTT	−7.0	−6.6	2.0	1.7	7.5	14 (3–17)
Mean all sites	−4.3	−5.7	2.2	1.6	–	–

* Minimum value of −5 cm for Okarito indicates that cluster roots were 5 cm below the standing water table at the bog surface.

(NIWA) National Climate Database (cliflo.niwa.co.nz; data accessed May 2014). The $0.05° × 0.05°$ gridded Virtual Climate Station Network (VSCN; Tait et al., 2006, 2012) cells containing each of our sites were used to calculate long term annual or growing season means, or sums for precipitation, from 1972 to 2013.

To examine spatial variation in the isotopic composition of precipitation we used isoscape modelled values for $\delta^{18}O$ and δD from the VSCN grid square containing each of our sites. The isoscape model is based on $\delta^{18}O$ and δD measurements of monthly precipitation samples collected between 2007 and 2009 from 51 sites across NZ (Frew and Van Hale, 2011), which were used to develop a multiple linear regression model (including two geographic and five daily meteorological VSCN variables; Ehtesham et al., 2013). All meteorological variables were weighted by daily precipitation amounts to generate monthly-weighted climate means corresponding to the collection times of the precipitation samples. These weighted means, as well as latitude and elevation, were regressed, using JMP v.8 (SAS Institute, North Carolina, USA), against all available monthly $\delta^{18}O$ and δD observations using stepwise backward elimination, supervised to eliminate highly correlated variables (regression statistics and equation in Table S1). VCSN climate data were then used with the final regression equation to calculate an estimate of daily- and monthly-weighted precipitation δD and $\delta^{18}O$ for each point on the $0.05 × 0.05°$ grid, processed in Matlab R2012b (The Mathworks, Massachusetts, USA). The modelling and mapping procedure was validated by Ehtesham et al. (2013).

GNIP (Global Network of Isotopes in Precipitation) data for $\delta^{18}O$ and δD in precipitation from Kaitaia (1972–1991) and Invercargill (1977–1991; IAEA/WMO, 2014; data accessed July 2014) provided a lower resolution check on the isoscape data.

NOAA (US National Oceanic and Atmospheric Administration) HYSPLIT (HYbrid Single Particle Lagrangian Integrated Trajectory; Draxler and Rolph, 2014) back-trajectory models were run to examine precipitation moisture source regions over the course of the year-long temporal dataset at KOP. We modelled air mass trajectory for the 72 h before the rain day (>5 mm day^{-1}) prior to each sampling day. We used trajectory type 1 (ensemble), the GDAS global archived meteorological dataset (2006 – present) and a level height of 250 m above ground level.

2.3. $\delta^{18}O$ and δD analyses

Root and shoot samples were prepared to α-cellulose using a standard methodology (Loader et al., 1997; Daley et al., 2010). Roots were cleaned with distilled water and manually separated from other plant material; each sample was wet-sieved to remove fine detritus and all other plant remains then removed using a low-powered microscope at ×10 magnification. Roots and shoots were cut into short (approximately 1 mm) sections prior to chemical treatment (bleaching). Five 1 h bleaching stages were sufficient to form pure white cellulose for the root samples (Daley et al.,

2010), but up to 10 equivalent bleaching stages were required for shoot samples to obtain a product of similar visual purity.

Oxygen ($\delta^{18}O$) and hydrogen (δD) stable isotope ratios of water samples were measured at the Lancaster Environment Centre (LEC), Lancaster University, UK, using a Vario Pyrocube with Vario Liquid Autosampler (Elementar Analysensysteme, Germany), interfaced with an Isoprime 100 isotope ratio mass spectrometer (Isoprime, UK) set in continuous flow mode. All water samples were filtered prior to analysis to remove small quantities of particulates introduced to the sample during collection. For δD, 1 µl of water was reduced to hydrogen gas at 1080 °C over a chrome-based catalyst. $\delta^{18}O$ was determined by pyrolysis of 0.5 µl of water at 1450 °C over glassy carbon. Internal (LEC tap water #2) and international standards (VSMOW, GISP) were run with each batch of samples with analytical precision typically better than 0.4‰ and 1‰ and for $\delta^{18}O$ and δD respectively.

Oxygen ($\delta^{18}O$) and hydrogen (δD) stable isotope ratios of cellulose samples were measured at Swansea University, UK, following the simultaneous COH method described by Loader et al. (2014). Samples of 300–350 mg dried α-cellulose were passed from an autosampler (Filot et al., 2006) into an equilibration chamber heated to 110 °C, through which steam of known isotopic composition (IAEA-CH7 and IAEA-C3) was passed in a flow of helium. Samples were left to equilibrate for 600 s, dropped into a Flash HT elemental analyser (Thermo GmbH, Germany) and pyrolysed over glassy carbon at 1400 °C prior to mass-spectrometric analysis using a Thermo Delta V mass spectrometer (Thermo GmbH, Germany). IAEA-CH7 standards were run with each batch of samples. Standard precision was ±0.30‰ and ±3.0‰ for $\delta^{18}O$ and δD respectively (Loader et al., 2014).

Stable oxygen ($\delta^{18}O$) and hydrogen (δD) isotope ratios were reported as permil (‰) deviations from the VSMOW standard where:

$$\delta^{18}O \quad \text{or} \quad \delta D \, (‰) = \frac{R_{\text{sample}}}{R_{\text{standard}}} - 1 \quad \text{(Coplen, 2011)} \tag{1}$$

where R is the ratio of $^{18}O/^{16}O$ or $^2H(D)/^1H$ in the sample and standard. A mean of three isotope measurements was calculated for each sample. Since neither $\delta^{18}O$ or δD are independent variables, all water lines presented in $\delta^{18}O/\delta D$ biplots (Fig. 2) are calculated using Deming regression, a form of orthogonal linear regression which assumes error for both x and y variables.

3. Results

3.1. Precipitation and cellulose source water

Mean annual $\delta^{18}O$ in precipitation from isoscape modelled data for NZ and GNIP sites at Kaitaia and Invercargill provided an indication of the spatial variability in the isotopic composition of precipitation (Table 1, Fig. 1). Strong gradients exist that represent source and temperature effects on $\delta^{18}O$ (Barbour, 2007), with more
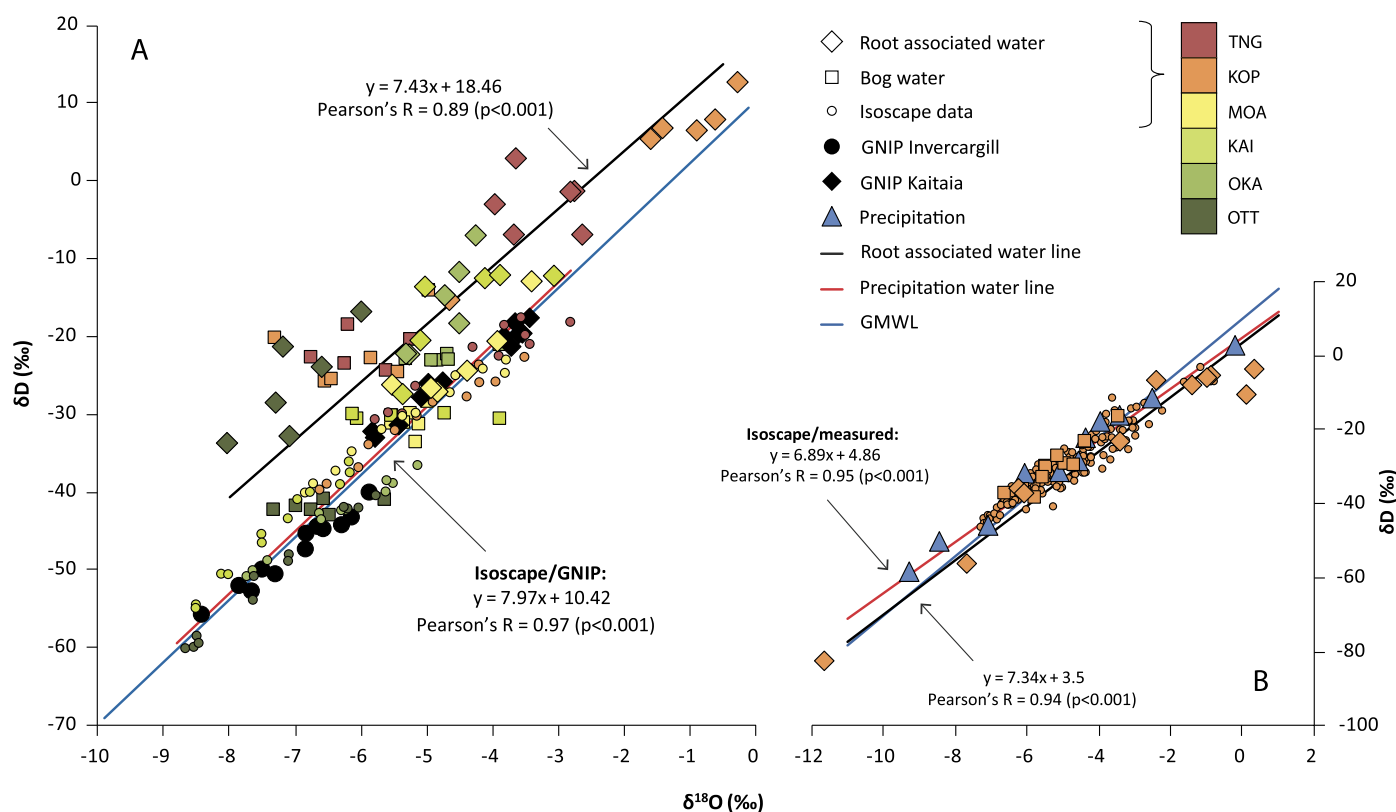
Fig. 2. (A) $\delta^{18}O/\delta D$ biplot of mean monthly 1997–2013 isoscape modelled precipitation from all sites and GNIP data from Kaitaia and Invercargill compared to root-associated water and bog water samples from all sites in the spatial dataset. Global meteoric water line (GMWL; blue) and a local meteoric line derived from the combined isoscape and GNIP data (red) are shown. (B) $\delta^{18}O/\delta D$ biplot of mean monthly 1997–2013 isoscape modelled precipitation from all sites and monthly measured precipitation compared to root-associated water and bog water (means of two monthly replicate values are plotted for root-associated and bog water) samples from KOP in the temporal dataset. GMWL = global meteoric water line. For (A) and (B), Pearson's r values are given for the correlation between $\delta^{18}O$ and δD for the relevant datasets. (For interpretation of the references to colour in this figure legend, the reader is referred to the web version of this article.)

^{18}O enriched values occurring in the Northland and Waikato regions where a warmer climate is more influenced by sub-tropical moisture sources and more ^{18}O depleted values in the South Island where a cooler climate is more dominated by the prevailing southern ocean westerly winds. GNIP data support this general pattern with precipitation from the southerly, cooler Invercargill being more ^{18}O depleted than Kaitaia precipitation (Table 1). Site-specific isoscape data show more ^{18}O enriched values for TNG, KOP and MOA, with OKA and OTT more ^{18}O depleted (Table 1). In addition, altitude (more ^{18}O depleted values with increasing altitude) and, to a lesser extent, rainout (progressively more ^{18}O depleted precipitation moving inland from the coast) effects also contribute to the overall variability in $\delta^{18}O$ observed, particularly at KAI (Fig. 1). A local meteoric water line (LMWL) for NZ derived from the combined isoscape and GNIP datasets is highly significant ($r = 0.97$, $p < 0.001$) and conforms to the global meteoric water line (GMWL) with a slope of 7.97 (Fig. 2A).

Full results for root-associated and bog water $\delta^{18}O$ for the spatial and temporal datasets are given in Tables S2 and S3. In the spatial dataset, root-associated water $\delta^{18}O$ and δD are significantly positively correlated ($r = 0.89$, $p < 0.001$) and also broadly conform to the expected pattern along the GMWL with waters from the warmer, lower latitude North Island sites generally positioned higher compared to the cooler, higher latitude South Island sites (Fig. 2A). Waters from KOP and TNG are the most ^{18}O and D enriched, suggesting evaporative enrichment at these sites, with more overlap and a less clear gradient between the remaining sites, though, on average, water from OTT is the most ^{18}O and D depleted. A water line derived from root-associated waters is broadly parallel to (slope of 7.43), but offset above the GMWL and LMWL.

This offset is primarily driven by three sites (TNG, OKA and OTT), whereas root-associated waters at KOP, MOA and KAI are more consistent with the slope and intercept of the LMWL (Fig. 2A). Mean site root-associated water and isoscape precipitation values are strongly positively correlated but this is not significant ($r = 0.689$, $p = 0.13$).

Bog water $\delta^{18}O$ and δD values from the spatial dataset are significantly but weakly positively correlated ($r = 0.384$, $p = 0.02$) and occur over a much narrower range of values than the root-associated water samples, suggesting that bog water is more isotopically homogeneous. The weak response of bog water to the isotopic composition of precipitation is also evident in its relationship to latitude. Whereas root-associated water shows a clear ^{18}O depletion effect with increasing southerly latitude (significant negative correlation $r = -0.72$, $p < 0.001$), bog water values remain relatively stable across the latitudinal gradient sampled ($r = -0.11$, $p = 0.53$).

In the temporal dataset, root-associated water and bog water $\delta^{18}O$ and δD are both significantly correlated (root-associated water $r = 0.94$, $p < 0.001$; bog water $r = 0.80$, $p < 0.001$) and water lines conform to the slope and intercept of the measured and isoscape-modelled precipitation (Fig. 2B), as well as the GMWL, without the offset evident in the spatial dataset (Fig. 2A). Root-associated water $\delta^{18}O$ co-varied strongly with precipitation over the year of sampling whereas bog water again showed less variability, with bog water values occurring over a narrower range (Fig. 3B). Furthermore, while both root-associated and bog water were positively correlated with precipitation, r values were higher for root-associated water–precipitation ($r = 0.85$, $p < 0.001$) and the bog water–precipitation relationship was not significant at

Table 3
Rainfall events prior to sampling days in the temporal dataset at KOP for which NOAA HYSPLIT back trajectory models were run to determine precipitation moisture source. Precipitation and wind data are from climate station within 100 metres of sampling points (see Section 2.1). Moisture source regions are defined *sensu* Sturman and Tapper (2006). See also Fig. S1.

Sampling date	Date of previous rainfall event	Rainfall amount (mm)	Wind direction on rain day (°)	Wind compass	Moisture source region
08/11/2012	29/10/2012	6.9	128	SE	Tropical maritime Tasman
11/12/2012	06/12/2012	12.4	269	W	Tropical maritime Pacific
11/01/2013	30/12/2012	6.3	247	WSW	Tropical maritime Pacific
08/02/2013	05/02/2013	7.7	241	WSW	Tropical maritime Pacific
12/03/2013	03/03/2013	3.2	244	WSW	Southern maritime
09/04/2013	05/04/2013	10.6	172	S	Southern maritime
22/05/2013	21/05/2013	7.3	156	SSE	Tropical maritime Pacific
11/06/2013	09/06/2013	47.7	144	SE	Modified Polar maritime
23/07/2013	14/07/2013	9.3	170	S	Modified Polar maritime
21/08/2013	19/08/2013	12.0	162	SSE	Modified Polar maritime
27/09/2013	24/09/2013	42.6	139	SE	Tropical maritime Tasman
05/11/2013	31/10/2013	18.5	279	W	Tropical maritime Pacific

$\alpha = 0.05$ ($r = 0.55$, $p = 0.08$). The root-associated water samples from the summer months (Dec.–Apr.) were more ^{18}O enriched than most of the precipitation values from the same period, suggesting that evaporative enrichment was occurring (Fig. 3B). This is also evident as an evaporative trend from the GMWL at more enriched values (Fig. 2B).

Previous work on *Sphagnum* peatlands has shown that microtopography can have a significant effect on evaporative enrichment, leading to variability in source water for mosses growing at different points along a hummock to hollow gradient (Ménot-Combes et al., 2002). Although microtopographical variation on *Empodisma* peatlands is less than typically observed on *Sphagnum* peatlands, we tested whether this had any effect at our sites. There were no significant correlations between water-table depth and root-associated or bog water for either δ^{18}O or δD although the δ^{18}O variability in root-associated water (7.75‰) was greater than reported in surface waters across a hummock to hollow gradient in a *Sphagnum* peatland (4‰; Ménot-Combes et al., 2002). Mean site δ^{18}O and δD values for root-associated water were consistently more ^{18}O and D enriched and showed more variability than mean site values for bog water, suggesting a degree of evaporative enrichment in root-associated waters and a dampening of the precipitation signal in bog waters (Table 2). Neither of these effects were related to water-table depth. The difference between bog and root-associated waters was highest in the warmer northern sites of KOP and TNG, whereas other sites had more similar or overlapping bog and root-associated water ranges, suggesting that the evaporative effect is highest in the northern, warmer sites, but is unrelated to water-table depth.

To examine the different moisture sources for precipitation over the year of sampling at KOP, we ran HYSPLIT back-trajectory models (Draxler and Rolph, 2014) for the rain days (>5 mm day^{-1}) prior to each sampling day and characterised moisture source regions *sensu* Sturman and Tapper (2006) in Table 3. Tropical moisture source regions are characterised by a more heavy isotope enriched signature, whereas those with a more distant, cooler southerly moisture source originating in the Southern Ocean are characterised by a more heavy isotope depleted signature. It is clear from both the wind direction and moisture source regions that there is a seasonal shift in weather patterns delivering precipitation to KOP over the year, with more westerly winds and tropical moisture sources dominating during the summer months and more southerly winds and southern/polar moisture sources dominating during the winter months. This is reflected in both the precipitation and root-associated water results in the temporal dataset (Fig. 3) which show more ^{18}O and D enriched values when tropical moisture sources were dominant and relatively ^{18}O and D depleted values when southern/polar moisture sources were dominant.
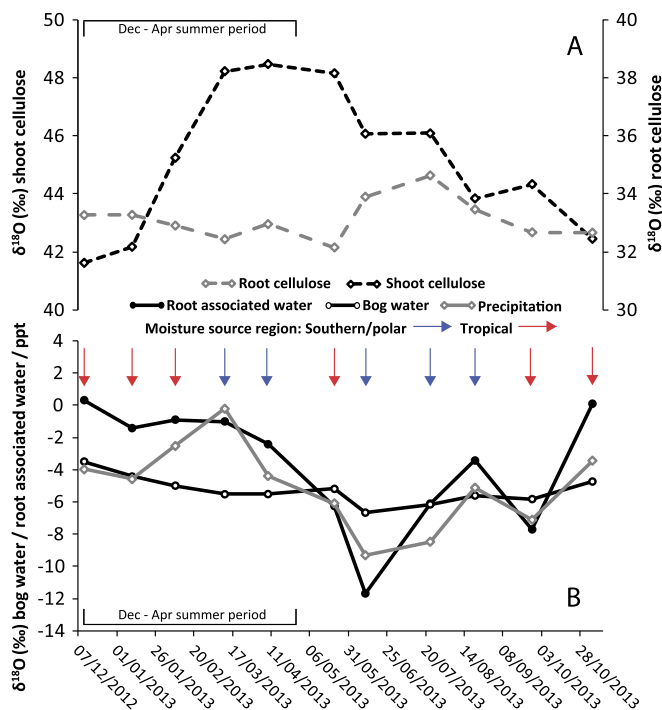

Fig. 3. (A) δ^{18}O in root and shoot cellulose. Note different y axis scales. (B) δ^{18}O in root-associated water, bog water and precipitation with indication of precipitation moisture source. Data in both panels as measured from monthly samples taken at KOP from November 2012 to November 2013. For root and bog waters and root and shoot cellulose, the values plotted are means of results from two sampling locations. Sampling dates and moisture source regions are shown in Table 3. For a full colour version of this figure, the reader is referred to the web version of this article

3.2. Source waters and plant cellulose

Full results for *Empodisma* root and shoot δ^{18}O$_C$ for the spatial and temporal datasets are given in Tables S4 and S5. Shoot δ^{18}O$_C$ values were consistently higher than root δ^{18}O$_C$ (Fig. 3A; mean = 39.7 ± 2.4‰ (1σ) for shoots versus 31.3 ± 0.9‰ for roots in the spatial dataset ($n = 36$) and 44.9 ± 2.7‰ for shoots versus 33 ± 1‰ for roots in the temporal dataset ($n = 24$)). The wide range of δ^{18}O$_C$ values (3.3‰ and 8‰ for spatial roots and shoots and 3.3‰ and 9‰ for temporal roots and shoots respectively) reflected the wide range of values for the isotopic composition of precipitation both over the site transect and the year of sampling (Table 1). The difference in magnitude of permil variation between roots and shoots may be a genuine reflection of relative source water values if internal shoot water is more evaporatively enriched than

Table 4

Correlation coefficients (*r* values) for $\delta^{18}O$ root and bog water with root and shoot cellulose. *p* values <0.1 are shown in parentheses. Spatial dataset correlations are for mean $\delta^{18}O$ of 6 site within site replicates for water and cellulose samples and GPP-weighted annual mean values for precipitation (see Section 3.3 for details). Temporal correlations are for mean $\delta^{18}O$ of two monthly replicate measurements for water and cellulose samples. Precipitation was collected for 11 months.

		Root cellulose $\delta^{18}O$	Shoot cellulose $\delta^{18}O$	*n*
Spatial dataset	Root water	−0.278	−0.068	6
	Bog water	−0.274	−0.498	6
	Precipitation	−0.124	−0.019	6
Spatial dataset (without KAI)	Root water	−0.487	−0.141	5
	Bog water	−0.148	−0.481	5
	Precipitation	−0.911 (0.032)	−0.603	5
Temporal dataset	Root water	−0.405	−0.153	12
	Bog water	−0.379	−0.464	12
	Precipitation	−0.597 (0.053)	0.043	11

internal root water when cellulose synthesis takes place, or may only reflect sampling regime (see below). Root, and particularly shoot, $\delta^{18}O_C$ values were significantly higher than those reported for other peatland vascular plants (e.g. 27–30‰, Brenninkmeijer et al., 1982; about 24‰, Ménot-Combes et al., 2002; 20–25‰, Hong et al., 2009). Mean $\delta^{18}O_C$ values for the samples of other vascular plants growing at our sites ($n = 20$) were also higher than previous studies at 30.7‰ ± 2.4‰ (1σ), equivalent to *Empodisma* spp. root $\delta^{18}O_C$, but again much lower than shoot $\delta^{18}O_C$ (Table S6).

Root-associated or bog water and root or shoot $\delta^{18}O_C$ were not significantly correlated in either the spatial or temporal datasets (Table 4), though in the temporal dataset, precipitation and root cellulose were relatively strongly negatively correlated, which was almost significant at $\alpha = 0.05$ ($r = -0.59$, $p = 0.053$). When KAI was removed from the spatial dataset as a potential outlier (Section 2.1), a strong and significant negative correlation between precipitation and root cellulose was evident ($r = -0.911$, $p = 0.032$; Table 4). Fig. 4 further supports the strong negative correlation be-
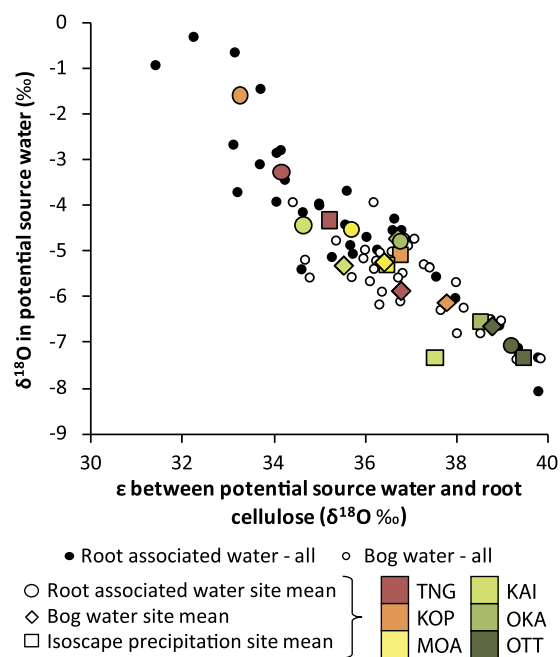

Fig. 4. Epsilon/water biplot of $\delta^{18}O$ in potential source waters (precipitation, root-associated water, bog water) with enrichment (ε) between potential source water and root cellulose for the spatial dataset. For root-associated water and bog water, means are of six within site replicates, for precipitation, 1997–2013 mean monthly values are used. For a full colour version of this figure, the reader is referred to the web version of this article

tween source waters and cellulose, with higher ε where source water is more ^{18}O depleted.

However, $\delta^{18}O/\delta D$ biplots for the spatial (Fig. 5A) and temporal (Fig. 5B) datasets show that cellulose values were considerably more scattered than root-associated water and precipitation. In the temporal dataset, outlying values occurred in both the summer and winter months suggesting a lack of obvious seasonality
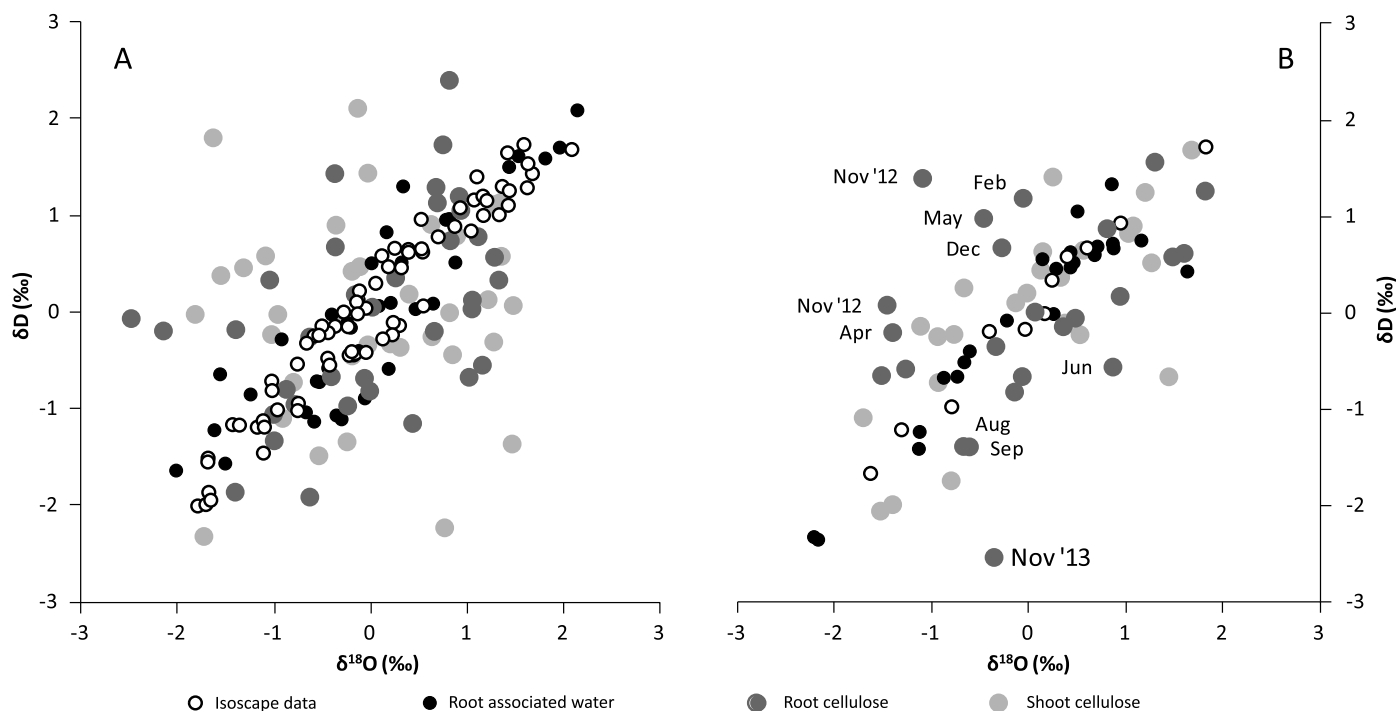

Fig. 5. $\delta^{18}O/\delta D$ biplots (standardised *z*-scores) of the isotopic composition of precipitation (mean monthly 1997–2013 values from the modelled isoscape data for spatial dataset, measured precipitation for temporal dataset; open circles), root-associated water (closed circles), root cellulose (dark grey circles) and shoot cellulose (light grey circles) for (A) the spatial dataset and (B) the temporal dataset. Outlying root cellulose values in (B) are labelled with sampling month.
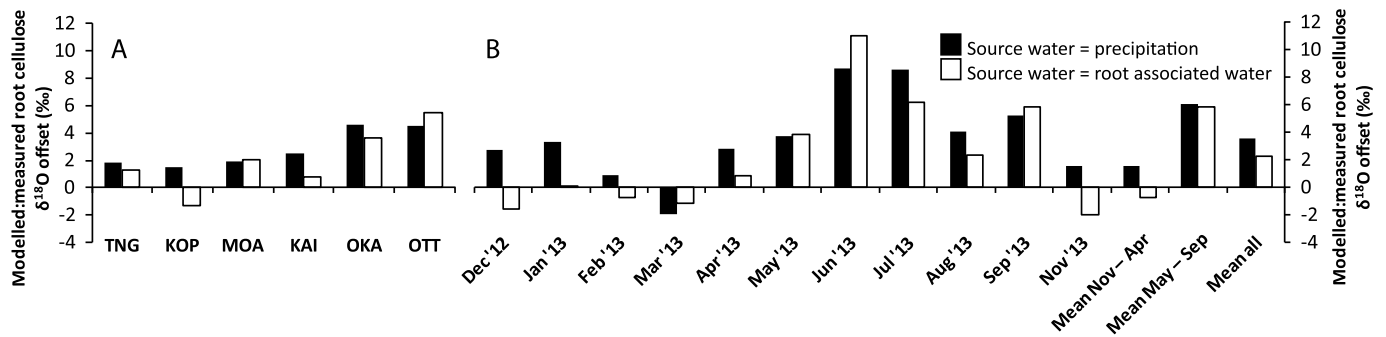
Fig. 6. $\delta^{18}O$ offset (‰) between measured and modelled root cellulose values for the spatial (A) and temporal (B) datasets. Site names are defined in Section 2.1. Black bars = source water in model is precipitation; white bars = source water in model is root-associated water.

in the discrepancy between cellulose and source water values. In the temporal dataset (Fig. 3), shoot cellulose broadly tracked root-associated water and precipitation, with more ^{18}O enriched values in late summer (March and April) and a decline to more ^{18}O depleted values over the winter months. Conversely, root cellulose $\delta^{18}O$ showed an antiphase relationship with precipitation and root-associated water, with relatively ^{18}O depleted values in the summer months when source waters were more ^{18}O enriched and an apparent ^{18}O enrichment of root cellulose in the winter months when source waters were more ^{18}O depleted, though the variation of root cellulose values occurred over a narrower permil range when compared to shoot cellulose. This disconnect between shoot and root cellulose may partly reflect sampling regime. Shoot samples were formed from well-defined recent growth that reflected monthly precipitation variation, as the cellulose was newly synthesised, whereas the root cellulose, extracted from samples in which new growth was difficult to precisely delineate, reflected a longer-term average of source water inputs.

3.3. Mechanistic modelling

A mechanistic model was applied to predict $\delta^{18}O_C$ from $\delta^{18}O_{SW}$, relative humidity and the equilibrium (ε_e), kinetic (ε_k) and biochemical (ε_b) fractionation processes. A range of models have been presented by different authors (e.g. Ménot-Combes et al., 2002; Waterhouse et al., 2002; Zanazzi and Mora, 2005; Barbour, 2007; Daley et al., 2010; Yu et al., 2011; Yu, 2013). Such models have been criticised due to their simplicity (Barbour, 2007) but are used here since more detailed physiological models require input values for processes for which measurements were not available. Despite minor differences in form, the general approaches of these models are similar and are summarised by Zanazzi and Mora (2005) and Daley et al. (2010) as (definitions of all terms in Table S7):

$$\delta^{18}O_C = \delta^{18}O_S + \varepsilon_b + (\varepsilon_e + \varepsilon_k)(1 - h) \qquad (2)$$

where

$$\varepsilon_e = \left[\exp\left(\frac{1137}{T^2} - \frac{0.4156}{T} - 0.0020667 \right) - 1 \right] \times 1000 \quad \text{(Yu, 2013)} \qquad (3)$$

Calculated values for ε_e for each site (Eq. (3), Table S8) were consistent with those produced using globally distributed GNIP data for temperatures between 15 and 20 °C (10.3‰ at 15 °C to 9.8‰ at 20 °C) by Araguas-Araguas et al. (2000). Equation (2) assumes equilibrium between source water and atmospheric water vapour. This was assumed for the growing season in central Europe (Ménot-Combes et al., 2002) and is a reasonable assumption in our case given the demonstrated correlation between precipitation and root-associated water. Kinetic fractionation occurs during

transpiration and is dependent on the relative humidity over the evaporating surface and the airflow dynamics in the leaf boundary layer, which is controlled by leaf size and morphology, with plants with smaller, segmented leaves having a lower component of turbulence, resulting in higher ε_k values (Buhay et al., 1996; Araguas-Araguas et al., 2000). Several different values have been published for ε_k ranging from 16‰ for a turbulent boundary layer (Dongmann et al., 1974; Yu et al., 2011) to 28‰ for a stagnant boundary layer (e.g. Aucour et al., 1996; Ménot-Combes et al., 2002). Buhay et al. (1996) present a range of 18.4 ± 6.1‰, dependent primarily on leaf morphology. Given the scale-like leaves and high water use efficiency of *Empodisma* spp. (Wagstaff and Clarkson, 2012), we used the upper limit of 28.5‰ for ε_k, *sensu* Ménot-Combes et al. (2002). We use the ± 3‰ error associated with biochemical fractionation (Yakir and DeNiro, 1990; Table S7) to assess whether model predicted $\delta^{18}O$ is an accurate reflection of measured $\delta^{18}O$.

We used mean annual temperature for TNG, KOP and MOA as these sites have year round growing seasons (e.g. Campbell et al., 2014; Goodrich et al., 2015) and mean November to March temperature for KAI, OKA and OTT to represent the shorter growing season in these locations. To reflect these differences and better represent the seasonality of *Empodisma* spp. growth, we used a gross primary productivity (GPP) weighted mean of precipitation $\delta^{18}O$. This was calculated by using the strong, significant relationship between monthly air temperature and GPP at KOP (monthly measurements from October 2012 to January 2014; $r = 0.9$, $p < 0.001$; Fig. S2) to predict monthly GPP at all sites based on mean monthly (1972–2013) NIWA VSCN temperature data. We then used monthly proportions of total annual GPP and isoscape modelled mean monthly precipitation $\delta^{18}O$ to calculate a GPP-weighted mean annual value for precipitation $\delta^{18}O$ at each site.

For both the spatial (Table S8) and temporal (Table S9) datasets, using root-associated water rather than precipitation as the source water for cellulose synthesis resulted in predicted $\delta^{18}O$ values closer to measured $\delta^{18}O$ on average (Fig. 6), though in the spatial dataset, both potential water sources resulted in mean offsets less than the 3‰ error associated with biochemical fractionation. That root-associated water is a marginally better predictor of $\delta^{18}O_C$ may support the earlier assertion that, despite the low levels of evaporation from the surface of *Empodisma*-dominated bogs (Campbell and Williamson, 1997), some degree of evaporative enrichment of precipitation has taken place in our root-associated water samples. Root-associated water was more ^{18}O enriched than precipitation at all sites with the exception of OTT. To further examine the relative roles of root-associated water and precipitation as potential source waters, we applied the mechanistic model to surface plant samples of the most common other vascular plant species at each site (Table S6) and a simplified model for mosses (Daley et al., 2010),

which excludes ε_e and ε_k, to *Sphagnum* samples taken at four sites (Table S10), where:

$$\delta^{18}O_{C(moss)} = \delta^{18}O_S + \varepsilon_b \qquad (4)$$

For both vascular plants and *Sphagnum*, mean modelled–measured offsets for both potential source waters fell within the $\pm 3\permil$ error range for biochemical fractionation (Tables S6 and S10), though root-associated water was once again a marginally better predictor of $\delta^{18}O_C$ than precipitation.

In the spatial dataset, using either root-associated water or precipitation as the input values for source water resulted in average modelled–measured offset for root $\delta^{18}O < 3\permil$. In both cases, the four North Island sites fell within this margin, whereas the two South Island sites had offset values $> 3\permil$ (Table S8; Fig. 6). The modelled–measured offset for shoot $\delta^{18}O$ was consistently higher (mean $= 10.31\permil$ for source water $=$ root-associated water) as a result of the much higher $\delta^{18}O_C$ for shoots compared to roots. In the temporal dataset (Table S9), the annual mean modelled–measured offset for root $\delta^{18}O$ (using root-associated water as the input value) was within acceptable error ($2.25\permil$), but the equivalent value for shoot $\delta^{18}O$ was again much higher ($14.28\permil$). Annual mean values hid distinct seasonality in the temporal data since offset values were consistently lower from November to April compared to the winter months (May to September; Table S9; Fig. 6).

4. Discussion: $\delta^{18}O$ relationships and development of a palaeoclimate proxy

The observed relationships between the isotopic composition of precipitation, root-associated water and bog water show that root-associated water reflects the isotopic composition of precipitation, and therefore the precipitation moisture source, over time and space (Fig. 2). Our first hypothesis is therefore upheld. Conversely, bog water, which represents a larger water volume, which is likely to have a longer turnover time than root-associated water, forms a more isotopically homogeneous pool in which the contemporary precipitation signal is dampened. This result is consistent with Ménot-Combes et al. (2002) who demonstrated, using short vertical profiles of $\delta^{18}O$ in a *Sphagnum*-dominated peatland, that water from depth was more isotopically homogeneous than surface water.

However, the relationships between precipitation/root-associated water and root/shoot cellulose were less clear (Table 4), meaning that our second hypothesis (that root cellulose reflects spatial and temporal variation in the source water) cannot currently be confidently upheld. Although we selected sites that have been defined as ombrotrophic in previous publications or display characteristics associated with ombrotrophy, the strong and significant negative relationship observed between precipitation and root cellulose in the spatial dataset when KAI was removed (Table 4) suggests that this site may be subject to external hydrological influences, most likely either surface run-off from surrounding upland slopes or heavy isotope depleted snowmelt, and may not therefore be fully ombrotrophic. The negative relationship between precipitation and root cellulose evident in the temporal and reduced spatial datasets (Figs. 3 and 4; Table 4) is in contrast to modelled predictions but may offer some insight into the link between source waters and cellulose. We propose two potential mechanisms that may explain this observation. Firstly, *Empodisma*-dominated peatlands have previously been described as a 'wet desert' (Campbell and Williamson, 1997), with large canopy resistance causing a hydrological separation of the dry shoots and wet roots, whereby new growth shoots in the upper canopy may become water-stressed even though roots below the canopy remain saturated. If shoots were most water-stressed in summer

months when source water is most enriched and stomata are only open for a relatively short part of the morning when evaporation potential is low (Sharp, 1995, quoted in Campbell and Williamson, 1997), there may be relatively less evaporative enrichment of leaf water, with the summer water signal more tightly impressed. In contrast, in winter when source water is more heavy isotope depleted, shoots may be less water-stressed and so assimilating with open stomata for longer periods, resulting in comparatively more evaporative enrichment, driving the observed negative correlation. Secondly, in winter months, when growth conditions may be marginal, shoots may remobilise stored starches from roots to form new sucrose. If this translocation favoured ^{16}O over ^{18}O, then roots would become more ^{18}O enriched and shoots more ^{18}O depleted, as observed (Fig. 3A). In order to drive the observed negative relationship, this hypothesis would be dependent on a low level of exchange occurring between organically bound oxygens with those in source water during photosynthesis. This figure has been estimated at 40–100% for the aquatic plant *Lemna gibba* under different growth conditions (Yakir and DeNiro, 1990), but the figure for *Empodisma* spp. specifically remains unknown. The absence of detailed physiological studies on, and understanding of, *Empodisma* spp. is therefore highlighted and must be addressed if its isotopic fractionation pathways are to be fully understood, in order to maximise the potential for palaeoclimate proxy development.

In both the spatial and temporal datasets, there was a narrower range of $\delta^{18}O$ values for root cellulose compared to root-associated water (spatial: root $\delta^{18}O_C$ range $= 3.3\permil$, root-associated water range $= 7.8\permil$; temporal: root $\delta^{18}O_C$ range $= 3.3\permil$, root-associated water range $= 14.4\permil$), an effect which has been previously observed along an altitudinal transect of bogs in Switzerland (Ménot-Combes et al., 2002). One possible explanation is that $\delta^{18}O_C$ values reflect an integrated longer-term average of more variable source water conditions over the growing season (Ménot-Combes et al., 2002), as the range is close to that observed for the site averages for precipitation ($3.02\permil$, Table 1). Furthermore, results from the modelling of temporal data showed better performance during the growing season, when active growth and cellulose synthesis effectively tracks changes in source water, which is also seen in the tracking of source waters by shoot cellulose in the temporal dataset (Fig. 3). Conversely, higher modelled-measured $\delta^{18}O_C$ values were observed during winter months (Table S9), when growth slows or ceases (Goodrich et al., 2015). However, rather than an effect of sensitivity, this seasonal differential in model performance for the temporal dataset may reflect the more negative $\delta^{18}O$ values for root-associated water and precipitation in the winter months, which are related to dominant polar (more ^{18}O depleted) moisture sources, as opposed to the dominant tropical (more ^{18}O enriched) moisture sources during the summer months (Table 3).

The observed relationship between root-associated water and precipitation is convincing in both spatial and temporal datasets. This, in addition to biochemical enrichment coefficients falling within error for the simplified modelling of *Sphagnum* cellulose samples (Table S10), suggests that root-associated water is a potential indicator of the internal leaf water. However, understanding the relationship between the external source water (i.e. root-associated water as measured here) and the internal water used in cellulose synthesis is essential for understanding the relationship between source water and plant cellulose. Measurements of $\delta^{18}O$ of extracted 'true' root and leaf water (e.g. by vacuum distillation; West et al., 2006) would allow the extent of any fractionation between external source water and internal root and leaf water to be quantified, but this was not undertaken in this study.

The good performance of the mechanistic modelling is partly dependent on the values calculated/used for different fractionation processes. Calculated values for ε_e fell within published ranges and ε_b is widely accepted and has been consistently applied at $27 \pm 3‰$ in many isotopic studies (e.g. Ménot-Combes et al., 2002; Waterhouse et al., 2002; Zanazzi and Mora, 2005; Daley et al., 2010; Yu et al., 2011; Yu, 2013). ε_k has the highest uncertainty with a value of $28.5‰$ chosen based on a review of literature and reasonable assumptions on the leaf form and physiology of *Empodisma* spp., but if kinetic fractionation was lower (e.g. Buhay et al., 1996 suggest a mean value of $18.4‰$) then modelled $\delta^{18}O_C$ values would fall outside of the $\pm 3‰$ error when compared to measured root $\delta^{18}O_C$. In addition, the broadly applied assumption of the temperature independence of ε_b has also recently been questioned (Sternberg and Ellsworth, 2011). Experiments generating cellulose at different temperatures showed that ε_b was consistent at a mean value of $26‰$ above temperatures of $20\,°C$ but increased below $20\,°C$ to up to $31‰$ (Sternberg and Ellsworth, 2011). Our sites are located in a climate space that spans similar temperature gradients (Table 1) so it may be reasonable to expect that ε_b is higher at the higher latitude, lower temperature sites (OKA and OTT). This would reduce the higher modelled–measured $\delta^{18}O$ offset seen for these sites in the spatial dataset (Table S8), resulting from higher mean root/shoot $\delta^{18}O_C$ at OTT and OKA compared to the North Island sites. Our data therefore lend tentative empirical support to the experimentally observed temperature dependence of ε_b and provide impetus for this issue to be addressed in field studies.

There was a consistent offset of mean value $10.2‰$ (range $6.1‰–16‰$) between root and shoot $\delta^{18}O_C$ across both spatial and temporal datasets, which may reflect the hydrological separation of shoots and roots caused by large canopy resistance (Campbell and Williamson, 1997). Mechanistic models predicted *Empodisma* spp. root, but not shoot, $\delta^{18}O_C$ values to within the error margin associated with biochemical fractionation, strengthening the case for root $\delta^{18}O_C$ as the primary target for proxy development. Results of mechanistic modelling indicate that improved understanding of oxygen isotope fractionation in *Empodisma*-dominated restiad peatlands could enable use of this approach as a new source of palaeoclimate data to reconstruct changes in past atmospheric circulation. However, our research has raised several important, as yet untested hypotheses regarding the plant physiology and isotopic fractionation of *Empodisma* spp., which should be addressed to enhance the potential of this proxy archive to provide valuable palaeoclimatic reconstructions in a climatically sensitive region lacking in other suitable proxies.

5. Conclusions

When oxygen stable isotope ratios are used as a proxy for past changes in new geographical or ecological contexts, it is critical that interpretation is empirically and mechanistically grounded and calibrated with modern climate data, with a clear understanding of the links between climate, source water and cellulose $\delta^{18}O$ values. To test the development of stable isotope palaeoclimate records from vascular plant-dominated peatlands, we sampled precipitation, surface and sub-surface waters and root and shoot plant material over spatial and temporal gradients in NZ. Variation in root-associated water tracked precipitation over both spatial and temporal gradients. The link between source water and plant cellulose was less clear, although mechanistic modelling predicted mean root $\delta^{18}O_C$ values within published error margins for both datasets. Improved understanding of *Empodisma* physiology and isotope fractionation should enable the development of this approach as a new source of palaeoclimate data to reconstruct changes in past atmospheric circulation.

Appendix A. Supplementary material

Supplementary material related to this article can be found online at http://dx.doi.org/10.1016/j.epsl.2015.08.015.

References

Agnew, A.D.Q., Rapson, G.L., Sykes, M.T., Bastow Wilson, J., 1993. The functional ecology of *Empodisma minus* (Hook, f.) Johnson & Cutler in New Zealand ombrotrophic mires. New Phytol. 124, 703–710.

Araguas-Araguas, L., Froehlich, K., Rozanski, K., 2000. Deuterium and oxygen-18 isotope composition of precipitation and atmospheric moisture. Hydrol. Process. 14, 1341–1355.

Aucour, A.-M., Hillaire-Marcel, C., Bonnefille, R., 1996. Oxygen isotopes in cellulose from modern and quaternary intertropical peatbogs: implications for palaeohydrology. Chem. Geol. 129, 341–359.

Barbour, M.M., 2007. Stable oxygen isotope composition of plant tissue: a review. Funct. Plant Biol. 34, 83–94.

Brenninkmeijer, C.A.M., van Geel, B., Mook, W.G., 1982. Variations in the D/H and $^{18}O/^{16}O$ ratio in cellulose extracted from a peat core. Earth Planet. Sci. Lett. 61, 283–290.

Brook, E.J., 2007. Ice core methods: stable isotopes. In: Encyclopedia of Quaternary Science, pp. 1212–1219.

Buhay, W.M., Edwards, T.W.D., Aravena, R., 1996. Evaluating kinetic fractionation factors used for ecologic and paleoclimatic reconstructions from oxygen and hydrogen isotope ratios in plant water and cellulose. Geochim. Cosmochim. Acta 60, 2209–2218.

Campbell, D.I., Williamson, J.L., 1997. Evaporation from a raised peat bog. J. Hydrol. 193, 142–160.

Campbell, D.I., Smith, J., Goodrich, J.P., Wall, A.M., Schipper, L.A., 2014. Year-round growing conditions explains large CO_2 sink strength in a New Zealand raised peat bog. Agric. For. Meteorol. 192–193, 59–68.

Cole, J.E., Rind, D., Webb, R.S., Jouzel, J., Healy, R., 1999. Climatic controls on interannual variability of precipitation $\delta^{18}O$: simulated influence of temperature, precipitation amount, and vapor source region. J. Geophys. Res., Atmos. 104, 14223–14235.

Coplen, T.B., 2011. Guidelines and recommended terms for expression of stable isotope-ratio and gas-ratio measurement results. Rapid Commun. Mass Spectrom. 25, 2538–2560.

Craig, H., Gordon, L.I., 1965. Deuterium and oxygen-18 variations in the ocean and the marine atmosphere. In: Tongiorgi, E. (Ed.), Stable Isotopes in Oceanographic Studies and Paleotemperatures. Consiglio Nazionale Delle Richerche, Spoleto, Italy, pp. 9–130.

Daley, T.J., Barber, K.E., Street-Perrott, F.A., Loader, N.J., Marshall, J.D., Crowley, S.F., Fisher, E.H., 2010. Holocene climate variability revealed by oxygen isotope analysis of Sphagnum cellulose from Walton Moss, northern England. Quat. Sci. Rev. 29, 1590–1601.

Daley, T.J., Mauquoy, D., Chambers, F.M., Street-Perrott, F.A., Hughes, P.D.M., Loader, N.J., Roland, T.P., van Bellen, S., Garcia-Meneses, P., Lewin, S., 2012. Investigating late Holocene variations in hydroclimate and the stable isotope composition of precipitation using southern South American peatlands: an hypothesis. Clim. Past 8, 1457–1471.

Dansgaard, W., 1964. Stable isotopes in precipitation. Tellus 16, 436–468.

Dongmann, G., Nürnberg, H.W., Förstel, H., Wagener, K., 1974. On the enrichment of $H_2^{18}O$ in the leaves of transpiring plants. Radiat. Environ. Biophys. 11, 41–52.

Draxler, R.R. Rolph, G.D. 2014. HYSPLIT (HYbrid Single-Particle Lagrangian Integrated Trajectory) model access via NOAA ARL READY website (http://www.arl.noaa.gov/HYSPLIT.php). NOAA Air Resources Laboratory, College Park, MD.

Ehtesham, E., Baisden, W.T., Keller, E.D., Hayman, A.R., Van Hale, R., Frew, R.D., 2013. Correlation between precipitation and geographical location of the δ^2H values of the fatty acids in milk and bulk milk powder. Geochim. Cosmochim. Acta 111, 105–116.

Elliot, M.B., 1998. Late Quaternary pollen records of vegetation and climate change from Kaitaia Bog, far northern New Zealand. Rev. Palaeobot. Palynol. 99, 189–202.

Filot, M.S., Leuenberger, M., Pazdur, A., Boettger, T., 2006. Rapid online equilibration method to determine the D/H ratios of non-exchangeable hydrogen in cellulose. Rapid Commun. Mass Spectrom. 20, 3337–3344.

Fletcher, M.-S., Moreno, P.I., 2012. Have the Southern Westerlies changed in a zonally symmetric manner over the last 14 000 years? A hemisphere-wide take on a controversial problem. Quat. Int. 253, 32–46.

Frew, R.D., Van Hale, R.J., 2011. A stable isotope rainfall map for the protection of New Zealand's biological and environmental resources. Report to New Zealand Ministry for Primary Industries, Biosecurity. 34 pp.

Gat, J.R., 2000. Atmospheric water balance – the isotopic perspective. Hydrol. Process. 14, 1357–1369.

Goodrich, J.P., Campbell, D.I., Schipper, L.A., Clearwater, M.J., Rutledge, S., 2015. Vapour pressure deficit is a critical climate control on GPP and the light response of NEE at a southern hemisphere bog. Agric. For. Meteorol. 203, 54–63.

Helliker, B.R., Richter, S.L., 2008. Subtropical to boreal convergence of tree-leaf temperatures. Nature 454, 511–515.

Hong, Y.T., Jiang, H.B., Liu, T.S., Zhou, L.P., Beer, J., Li, H.D., Leng, X.T., Hong, B., Qin, X.G., 2000. Response of climate to solar forcing recorded in a 6000-year δ^{18}O time-series of Chinese peat cellulose. Holocene 10, 1–7.

Hong, Y.T., Hong, B., Lin, Q.H., Shibata, Y., Zhu, Y.X., Leng, X.T., Wang, Y., 2009. Synchronous climate anomalies in the western North Pacific and North Atlantic regions during the last 14 000 years. Quat. Sci. Rev. 28, 840–849.

IAEA/WMO, 2014. Global network of isotopes in precipitation. The GNIP database. Accessible at: http://www.iaea.org/water.

Leng, M.J., 2004. Isotopes in quaternary palaeoenvironmental reconstruction (ISOPAL). Quat. Sci. Rev. 23, 739–741.

Loader, N.J., Robertson, I., Barker, A.C., Switsur, V.R., Waterhouse, J.S., 1997. An improved technique for the batch processing of small wholewood samples to α-cellulose. Chem. Geol. 136, 313–317.

Loader, N.J., Street-Perrott, F.A., Daley, T.J., Hughes, P.D.M., Kimak, A., Levanič, T., Mallon, G., Mauquoy, D., Robertson, I., Roland, T.P., van Bellen, S., Ziehmer, M.M., Leuenberger, M., 2014. Simultaneous determination of stable carbon, oxygen and hydrogen isotopes in cellulose. Anal. Chem. 87, 376–380.

Ménot-Combes, G., Burns, S.J., Leuenberger, M., 2002. Variations of ^{18}O/^{16}O in plants from temperate peat bogs (Switzerland): implications for paleoclimatic studies. Earth Planet. Sci. Lett. 202, 419–434.

Newnham, R.M., Lowe, D.J., 2000. Fine-resolution pollen record of late-glacial climate reversal from New Zealand. Geology 28, 759–762.

Newnham, R.M., de Lange, P.J., Lowe, D.J., 1995. Holocene vegetation, climate and history of a raised bog complex, northern New Zealand based on palynology, plant macrofossils and tephrochronology. Holocene 5, 267–282.

Nichols, J., Booth, R.K., Jackson, S.T., Pendall, E.G., Huang, Y., 2010. Differential hydrogen isotopic ratios of Sphagnum and vascular plant biomarkers in ombrotrophic peatlands as a quantitative proxy for precipitation—evaporation balance. Geochim. Cosmochim. Acta 74, 1407–1416.

Oldfield, F., 2001. A question of timing: a comment on Hong, Jiang, Lui, Zhou, Beer, Li, Leng, Hong and Qin. Holocene 11, 123–124.

Royles, J., Sime, L.C., Hodgson, D.A., Convey, P., Griffiths, H., 2013. Differing source water inputs, moderated by evaporative enrichment, determine the contrasting δ^{18}O$_{CELLULOSE}$ signals in maritime Antarctic moss peat banks. J. Geophys. Res., Biogeosci. 118, 184–194.

Sternberg, L., Ellsworth, P.F.V., 2011. Divergent biochemical fractionation, not convergent temperature, explains cellulose oxygen isotope enrichment across latitudes. PLoS ONE 6, e28040. http://dx.doi.org/10.1371/journal.pone.0028040.

Sturman, A.P., Tapper, N.J., 2006. The Weather and Climate of Australia and New Zealand, second edition. Oxford University Press, Melbourne.

Tait, A., Henderson, R., Turner, R., Zheng, X.G., 2006. Thin plate smoothing spline interpolation of daily rainfall for New Zealand using a climatological rainfall surface. Int. J. Climatol. 26, 2097–2115.

Tait, A., Sturman, J., Clark, M., 2012. An assessment of the accuracy of interpolated daily rainfall for New Zealand. J. Hydrol. (N.Z.) 51, 25–44.

Ummenhofer, C.C., England, M.H., 2007. Interannual extremes in New Zealand precipitation linked to modes of Southern Hemisphere climate variability. J. Climate 20, 5418–5440.

Vandergoes, M.J., Newnham, R.M., Preusser, F., Hendy, C.H., Lowell, T.V., Fitzsimons, S.J., Hogg, A.G., Kasper, H.U., Schluechter, C., 2005. Regional insolation forcing of Late Quaternary climate change in the Southern Hemisphere. Nature 436, 242–245.

Wagstaff, S., Clarkson, B., 2012. Systematics and ecology of the Australasian genus Empodisma (Restionaceae) and description of a new species from peatlands in northern New Zealand. PhytoKeys 13, 39–79.

Waterhouse, J.S., Switsur, V.R., Barker, A.C., Carter, A.H.C., Robertson, I., 2002. Oxygen and hydrogen isotope ratios in tree rings: how well do models predict observed values? Earth Planet. Sci. Lett. 201, 421–430.

West, A.G., Patrickson, S.J., Ehleringer, J.R., 2006. Water extraction times for plant and soil materials used in stable isotope analysis. Rapid Commun. Mass Spectrom. 20, 1317–1321.

Yakir, D., DeNiro, M.J., 1990. Oxygen and hydrogen isotope fractionation during cellulose metabolism in *Lemna Gibba* L. Plant Physiol. 93, 325–332.

Yu, S.-Y., 2013. Quantitative reconstruction of mid- to late-Holocene climate in NE China from peat cellulose stable oxygen and carbon isotope records and mechanistic models. Holocene 23, 1507–1516.

Yu, S.-Y., Kang, Z., Zhou, W., 2011. Quantitative palaeoclimate reconstruction as an inverse problem: a Bayesian inference of late-Holocene climate on the eastern Tibetan Plateau from a peat cellulose δ^{18}O record. Holocene 22, 405–412.

Zanazzi, A., Mora, G., 2005. Paleoclimatic implications of the relationship between oxygen isotope ratios of moss cellulose and source water in wetlands of lake superior. Chem. Geol. 222, 281–291.